Chinese Chemical Letters 32 (2021) 1017–1019

Contents lists available at ScienceDirect

Chinese Chemical Letters

journal homepage: www.elsevier.com/locate/cclet

Communication

Three-dimensional organic cage with aggregation-induced delayed fluorescence

Yingyuan Hu[a], Li Li[b], Xiaoxia Wang[a,*], Dongge Ma[b], Fei Huang[b,*]

[a] School of Materials Science and Engineering, Dongguan University of Technology, Dongguan 523808, China
[b] State Key Laboratory of Luminescent Materials and Devices, Institute of Polymer Optoelectronic Materials and Devices, South China University of Technology, Guangzhou 510640, China

ARTICLE INFO

Article history:
Received 12 July 2020
Received in revised form 6 August 2020
Accepted 24 August 2020
Available online 25 August 2020

Keywords:
Organic cage
Two-step reaction
Aggregation-induced emission
Delayed fluorescence
Good solubility

ABSTRACT

A new kind of emissive small-molecular organic cage has been developed *via* the combination of coupling and condensation reactions, which shows outstanding solubility, structural stability and potential spatial isomeric chirality. Interestingly, through the introduction of proper donor and acceptor units, this emissive organic cage is the first among organic cages to exhibit red aggregation-induced delayed fluorescence with photoluminescence emission at 603 nm. The finding not only expands the types of emissive small-molecular organic cages, but also represents an important step for further development of red delayed fluorescence materials with good solubility and aggregation-induced emission feature.

Three-dimensional organic cages stand in the spotlight owing to their extensive potential applications in a variety of fields such as gas storage, permanent porous materials, host–guest chemistry and so on [1]. In particular, in the field of optical applications, luminescent organic cages have become a new light-generating platform because of their novel and unique photophysical properties [2]. However, the development of such materials still needs to be further promoted, especially, such as small-molecular emissive organic cages that have high atomic economy. Compared with luminescent self-assembled metallacages [3] and large cage frameworks [4], simple small-molecular emissive organic cages show low-cost and attractive solution-processable characteristic that makes them easier to be prepared into thin films by high-throughput solution-processing technology, such as ink-jet printing and spin coating, which is very necessary for the preparation of cost-efficient electronic devices [5]. However, they have rarely been reported.

On the other hand, at present, two main types of emissive materials have been widely reported, that is, aggregation-caused luminescence quenching (ACQ) and aggregation-induced emission (AIE) materials. In comparison with ACQ molecules, AIE materials exhibit strong luminescence in neat films [6], which is more conducive to simplify the preparation process of devices, such as non-doped devices and even single-layer devices. Therefore, the development of kinetically stable and simple small-molecular emissive organic cages with AIE feature is meaningful and valuable.

Herein, we have successfully constructed a new kind of emissive small-molecular organic cage with outstanding solubility and structural stability, namely **3M**, through a simple two-step reaction, which showed expected AIE characteristic. More interestingly, **3M** simultaneously exhibited red thermally activated delayed fluorescence (TADF) with photoluminescence (PL) emission at 603 nm. The materials possessing TADF property have been identified as the most promising and cost-effective candidates for lighting/display devices [7]. In addition, the crystal structure showed that **3M** had potential spatial isomeric chirality. The development of this kind of luminescent organic cage not only expands the types of emissive small-molecular organic cages, but also represents an important step for the further development of red TADF materials with good solubility and AIE feature.

This new emissive small-molecular organic cage was facilely prepared based on the synthetic routes depicted in Scheme 1. The first step was one-pot cage-forming reaction based on palladium-catalyzed Buchwald–Hartwig coupling between the commercially available starting materials, bis(3-bromophenyl)methanone and bis(3-aminophenyl)methanone, which proceeded at 100 °C to obtain **3CO** in 10.6% yield. The second step was Knoevnagel condensation of **3CO** and malononitrile mediated by $TiCl_4$ and pyridine under reflux conditions for 5 h to afford the target

* Corresponding authors.
E-mail addresses: wangxx@dgut.edu.cn (X. Wang), msfhuang@scut.edu.cn (F. Huang).

https://doi.org/10.1016/j.cclet.2020.08.038
1001-8417/

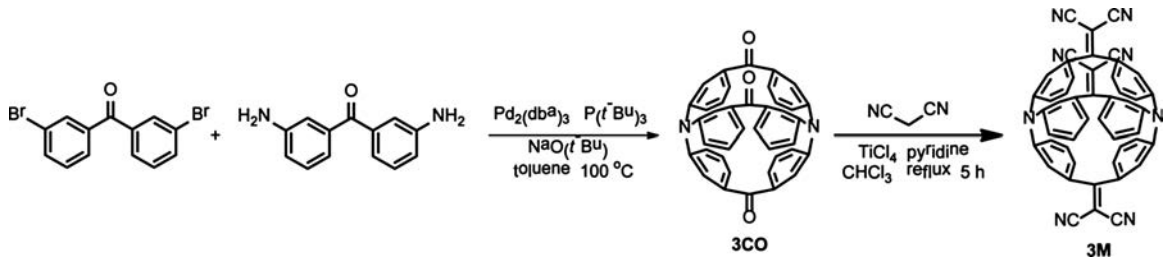

Scheme 1. Synthetic routes to target organic cage.

compound **3M** in 92% isolated yield). The structure of **3M** was identified by NMR spectroscopy, mass spectrometry, and single-crystal X-ray diffraction analysis, which also showed good structural stability with a decomposition temperature of up to 446 °C for **3M** (Fig. S1 in Supporting information).

The cage structure of **3M** with D_3 symmetry was confirmed by X-ray crystallography (Fig. 1a), which looked like a pretty clover with a fixed cavity, formed by the C-C distance of 6.980(15) Å and N-N distance of 5.539(96) Å. A regular triangle was formed by the three carbon atoms with each angle near 60°. Many solvent molecules can enter such a large cavity, potentially improving the solubility of **3M** (in fact generally >10 mg/mL in most solvents). Notably, analysis of the single crystal data of **3M** demonstrated the presence of two different configurations and indicated the existence of spatial isomeric chirality, which was further confirmed by the calculated mirror-image electronic circular dichroism spectra (Fig. 1b and Fig. S4 in Supporting information). From the side view, triphenylamine units (D) were formed on the upper and lower sides of **3M**. After combining with dicyanodistyrene units (A), a twisted D-A system was formed, which interestingly led to the realization of red TADF. Owing to that the spatial separation of the highest occupied molecular orbital (HOMO) and the lowest unoccupied molecular orbital (LUMO) can lead to a small singlet (S1)–triplet (T1) splitting energy (ΔE_{ST}), thus promoting reverse intersystem crossing (RISC) to realize effective TADF, the electronic and geometrical structures of **3M** were evaluated based on time-dependent density functional theory (TD-DFT) calculations. As shown in Fig. 1c, the HOMOs and LUMOs were mainly localized on the triphenylamine and dicyanodistyrene units, respectively, which resulted in a small calculated ΔE_{ST} value of 0.31 eV [7b,7c]. Meanwhile, the HOMOs and LUMOs were found to have weak overlap on the phenyl rings, which made **3M** realize effective light emission [8].

The steady-state UV–vis absorption and PL spectra of **3M** in toluene are shown in Fig. 2a. A weak absorption at *ca.* 415 nm was detected, which was assigned to the twisted intramolecular charge-transfer (TICT) transition and confirmed by the solvatochromic effect of PL with gradually red-shifted as increasing the polarity of the solvent (Fig. S5 in Supporting information). Upon photoexcitation, the solution exhibited structureless yellow emission with PL emission peak at 542 nm (Fig. 2a). The ΔE_{ST} value of **3M** was estimated to be 0.27 eV based on the onsets of the low-temperature fluorescence and phosphorescence spectra at 77 K in toluene (Fig. 2b), which was relatively small owing to the twisted cage structure and thus conducive to efficient RISC.

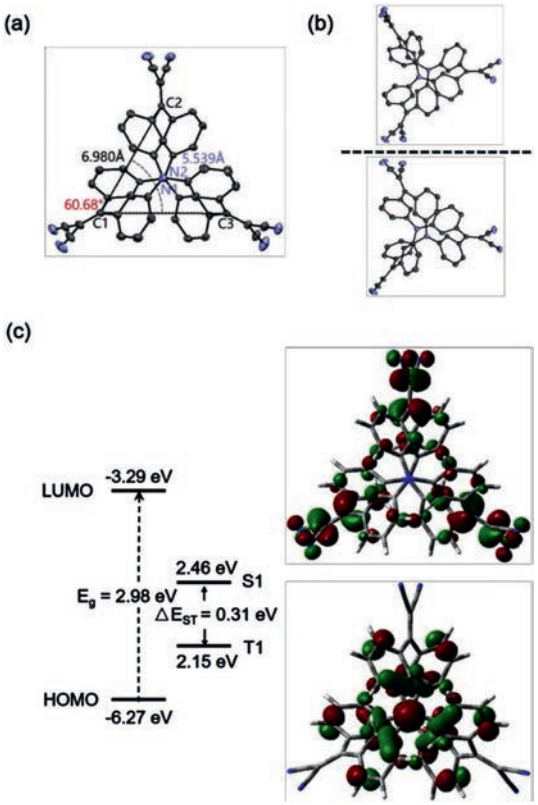

Fig. 1. (a) ORTEP drawing of **3M** from the side view. Hydrogen atoms are omitted for clarity. (b) Two different spatial isomers of **3M**. (c) HOMO and LUMO distributions, and calculated singlet (S1) and triplet (T1) energy levels of **3M** from the side view. The above calculations were conducted based on B3LYP/6-31 G(d) method.

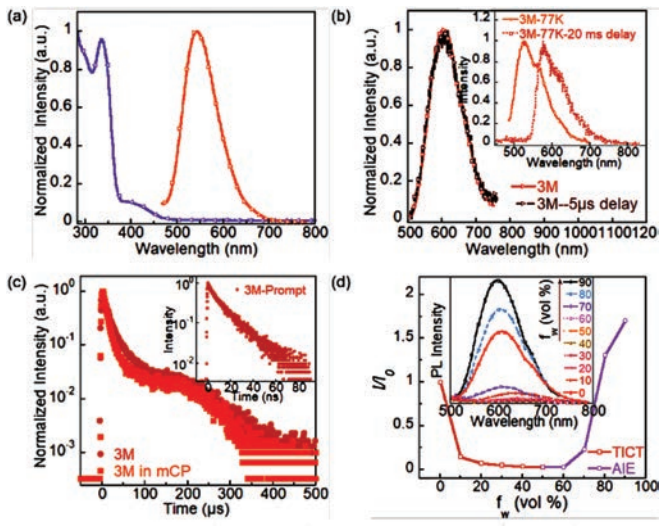

Fig. 2. (a) The UV–vis absorption and PL spectra for **3M** in toluene. (b) PL spectra of **3M** in neat film without delay time and with 5 μs delay time at room temperature. Inset: PL spectra of fluorescence and phosphorescence (delayed by 20 ms) for **3M** at 77 K in toluene. (c) Transient PL decay characteristics of **3M** in neat film and **3M**:mCP doped film under vacuum. Inset: Prompt emission decay curve. (d) Plot of *I* (emission intensity)/I_0 (emission intensity in THF solution) of **3M** *vs.* water fractions of the solvent mixture. Inset: PL spectra of **3M** (10^{-5} mol/L) in THF/water mixtures with different water fractions.

To further investigate the TADF property of **3M**, the time-resolved and temperature-dependent transient PL decays in neat film were carried out (Fig. 2c and Fig. S6 in Supporting information), which clearly exhibited both prompt and delayed fluorescence components at room temperature with lifetime (τ_p) of 14.9 ns and lifetime (τ_d) of 28.3 μs, respectively. The content of delayed fluorescence component under vacuum was more than that in air (Fig. S6 in Supporting information). Meanwhile, with the decrease of temperature from 300 K to 77 K, the content of delayed fluorescence component also decreased (Fig. S6). In addition, consistent prompt and delayed components with red PL emission at 603 nm in the time-dependent PL measurement implied that the delayed emission came from the same S1 state (Fig. 2b).

Interestingly, **3M** also presented the desirable AIE feature, which was confirmed by the emission behavior in THF/water mixtures with variable water volume ratio (f_w) (Fig. 2d). With the increase of f_w from 0% to 50%, the emission spectra and PL intensities gradually redshifted and decreased, which was due to the enhancement of TICT effect caused by the increase of solvent polarity [9]. As f_w continued to increase, the PL intensities increased dramatically with slight blue-shift in emission, which revealed the typical AIE characteristic of **3M** [10]. In addition, doped film of **3M** in a host material of 1,3-bis(carbazol-9-yl) benzene (mCP) (10 wt%) was prepared. From Fig. 2c, the delayed lifetime in the doped film (*i.e.*, 21.6 μs) was lower than that in neat film, reflecting that the delayed fluorescence was induced with aggregate formation (AIDF) [11]. On the other hand, an obvious decrease in the content of delayed fluorescence component from 300 K to 77 K was also observed from the temperature-dependent transient PL decays in the doped film, and the content of delayed fluorescence component in air was also less than that under vacuum, further confirming the TADF property of **3M** (Fig. S7 in Supporting information). The PL quantum yield (PLQY) in neat film (6%) was higher than those in the doped film and dilute solution (*i.e.*, 3% and 2%, respectively), which further verified its AIE feature. The PLQY value was not very high, which may be attributed to the weak electron-donating units. Due to the extreme distortion of the triphenylamine units, the conjugation effect was limited to some extent. It may be promising to achieve better performance towards brighter and redder luminescence such as by introducing electron-donating groups (*e.g.*, methoxy) to the benzene rings.

In conclusion, we have developed a new kind of simple emissive small-molecular organic cage **3M** *via* a facile two-step reaction, which exhibited excellent solubility, structural stability and potential spatial isomeric chirality. More interestingly, **3M** also showed red aggregation-induced delayed fluorescence, which was the first report of emissive organic cages with AIDF feature. We believe that this study will be meaningful not only to enlarge the research and types of luminescent small-molecular organic cages, but also to represent an important step for the further development of red TADF materials with high solubility and AIE characteristic.

Declaration of competing interest

The authors declare that they have no known competing financial interests or personal relationships that could have appeared to influence the work reported in this paper.

Acknowledgments

This work was financially supported by the National Natural Science Foundation of China (Nos. 51521002 and 21905048), the Foundation of Guangzhou Science and Technology Project (No. 201707020019), the Program for Science and Technology Development of Dongguan (No. 2019622163009), and the startup grants from Dongguan University of Technology for high-level talent (No. KCYKYQD2017018).

Appendix A. Supplementary data

Supplementary material related to this article can be found, in the online version, at doi:https://doi.org/10.1016/j.cclet.2020.08.038.

References

[1] (a) S.R. Seidel, P.J. Stang, Acc. Chem. Res. 35 (2002) 972–983;
(b) Y. Jin, C. Yu, R.J. Denman, W. Zhang, Chem. Soc. Rev. 42 (2013) 6634–6654;
(c) M.M.J. Smulders, I.A. Riddell, C. Browne, J.R. Nitschke, Chem. Soc. Rev. 42 (2013) 1728–1754;
(d) G. Zhang, M. Mastalerz, Chem. Soc. Rev. 43 (2014) 1934–1947;
(e) T. Hasell, A.I. Cooper, Nat. Rev. Mater. 1 (2016) 1–14;
(f) C.S. Diercks, O.M. Yaghi, Science 355 (2017) eaal1585;
(g) K. Sołtys-Brzostek, M. Terlecki, K. Sokołowski, J. Lewiński, Coord. Chem. Rev. 334 (2017) 199–231;
(h) D. Zhang, A. Martinez, J.P. Dutasta, Chem. Rev. 117 (2017) 4900–4942.
[2] (a) X. Yan, M. Wang, T.R. Cook, et al., J. Am. Chem. Soc. 138 (2016) 4580–4588;
(b) H. Qu, Y. Wang, Z. Li, et al., J. Am. Chem. Soc. 139 (2017) 18142–18145;
(c) H.T. Feng, Y.X. Yuan, J.B. Xiong, Y.S. Zheng, B.Z. Tang, Chem. Soc. Rev. 47 (2018) 7452–7476;
(d) H.T. Feng, X. Zheng, X. Gu, et al., Chem. Mater. 30 (2018) 1285–1290;
(e) X. Yan, P. Wei, Y. Liu, et al., J. Am. Chem. Soc. 141 (2019) 9673–9679.
[3] (a) X. Yan, T.R. Cook, P. Wang, F. Huang, P.J. Stang, Nat. Chem. 7 (2015) 342;
(b) M.L. Saha, X. Yan, P.J. Stang, Acc. Chem. Res. 49 (2016) 2527–2539;
(c) D.R. Martir, E. Zysman-Colman, Coord. Chem. Rev. 364 (2018) 86–117.
[4] (a) Y. Cui, B. Chen, G. Qian, Coord. Chem. Rev. 273 (2014) 76–86;
(b) Q. Gao, X. Li, G.H. Ning, et al., Chem. Commun. 54 (2018) 2349–2352;
(c) E. Jin, J. Li, K. Geng, et al., Nat. Commun. 9 (2018) 1–10;
(d) H. Kaur, S. Sundriyal, V. Pachauri, et al., Coord. Chem. Rev. 401 (2019) 213077;
(e) H.Q. Yin, F. Yin, X.B. Yin, Chem. Sci. 10 (2019) 11103–11109.
[5] X. Zheng, W. Zhu, C. Zhang, et al., J. Am. Chem. Soc. 141 (2019) 4704–4710.
[6] (a) Y. Hong, J.W.Y. Lam, B.Z. Tang, Chem. Soc. Rev. 40 (2011) 5361–5388;
(b) J. Mei, N.L.C. Leung, R.T.K. Kwok, J.W.Y. Lam, B.Z. Tang, Chem. Rev. 115 (2015) 11718–11940.
[7] (a) A. Endo, K. Sato, K. Yoshimura, et al., Appl. Phys. Lett. 98 (2011) 42;
(b) H. Uoyama, K. Goushi, K. Shizu, H. Nomura, C. Adachi, Nature 492 (2012) 234–238;
(c) Y. Tao, K. Yuan, T. Chen, et al., Adv. Mater. 26 (2014) 7931–7958;
(d) M.Y. Wong, E. Zysman-Colman, Adv. Mater. 29 (2017) 1605444;
(e) Z. Yang, Z. Mao, Z. Xie, et al., Chem. Soc. Rev. 46 (2017) 915–1016;
(f) T.T. Bui, F. Goubard, M. Ibrahim-Ouali, D. Gigmes, F. Dumur, Beilstein J. Org. Chem. 14 (2018) 282–308;
(g) X. Cai, S.J. Su, Adv. Funct. Mater. 28 (2018) 1802558;
(h) Y. Liu, C. Li, Z. Ren, S. Yan, M.R. Bryce, Nat. Rev. Mater. 3 (2018) 18020;
(i) S.K. Jeon, H.L. Lee, K.S. Yook, J.Y. Lee, Adv. Mater. 31 (2019) 1803524.
[8] (a) Q. Zhang, B. Li, S. Huang, et al., Nat. Photon. 8 (2014) 326;
(b) S. Hirata, Y. Sakai, K. Masui, et al., Nat. Mater. 14 (2015) 330–336.
[9] W. Rettig, Angew. Chem. Int. Ed. 25 (1986) 971–988.
[10] (a) Y. Dong, J.W.Y. Lam, A. Qin, et al., Appl. Phys. Lett. 91 (2007) 011111;
(b) J. Huang, N. Sun, Y. Dong, et al., Adv. Funct. Mater. 23 (2013) 2329–2337;
(c) Z.F. Chang, L.M. Jing, B. Chen, et al., Chem. Sci. 7 (2016) 4527–4536.
[11] (a) J. Huang, H. Nie, J. Zeng, et al., Angew. Chem. Int. Ed. 56 (2017) 12971–12976;
(b) J. Huang, Z. Xu, Z. Cai, et al., J. Mater. Chem. C 7 (2019) 330–339;
(c) C.M. Tonge, Z.M. Hudson, J. Am. Chem. Soc. 141 (2019) 13970–13976.